Received: 22 January 2020 | Revised: 14 April 2020 | Accepted: 16 April 2020

DOI: 10.1002/app.49370

ARTICLE

Journal of Applied Polymer Science WILEY

Impact of ultrasonication on carbon nanotube demixing and damage in polymer nanocomposites

Jayadurga Iyer Ganapathi[1] | Stephanie S. Lee[2] | Dilhan M. Kalyon[2,3] | Frank T. Fisher[1]

[1]Department of Mechanical Engineering, Stevens Institute of Technology, Hoboken, New Jersey

[2]Department of Chemical Engineering and Materials Science, Stevens Institute of Technology, Hoboken, New Jersey

[3]Department of Biomedical Engineering, Stevens Institute of Technology, Hoboken, New Jersey

Correspondence
Frank T. Fisher, Department of Mechanical Engineering, Stevens Institute of Technology, Hoboken, NJ 07030.
Email: frank.fisher@stevens.edu

Abstract

While ultrasonication is universally employed for dispersion and distribution of carbon nanotubes (CNTs) in a solvent or polymer solution, the current work focuses on the underlying mechanisms of CNT demixing and CNT damage that can occur during processing. Here, multi-walled CNTs were dispersed in a polycaprolactone polymer matrix using an established solution processing technique. Electrical, rheological, and mechanical characterization results suggest that once nanocomposite property enhancements reach an optimal level, further sonication leads to a decrease in the corresponding properties due to a combination of CNT damage and demixing mechanisms. Evidence of CNT damage from transmission electron microscopy, poor CNT distribution from optical image analysis and shear-induced crystallization results, and reagglomeration observed from ultraviolet–visible results, taken together, suggest that mechanisms of demixing and damage of the CNTs coexist for excessive sonication times.

KEYWORDS

mechanical properties, structure–property relationships, synthesis and processing techniques

1 | INTRODUCTION

The compounding of carbon nanotubes (CNTs) into polymers has the potential of generating functional nanocomposites that can be used in a wide range of applications. The success of incorporation of CNTs into a polymeric binder to achieve targeted functional end-use properties of the nanocomposite depends on the dispersion (agglomerate sizes) and distribution (spatial homogeneity) states of the CNTs within the nanocomposite. There are several processing techniques that can be used to incorporate CNTs into a polymeric binder. Such processing methods include ultrasonication, internal batch mixers, extruders, or in situ polymerization methods.[1,2] Although there are many different methods of processing to mix CNTs into a polymeric binder, it is still a significant challenge to successfully disentangle the as-received CNTs and to manipulate the dynamics of the formation of percolating networks of CNTs using conventional processing techniques.[1,3,4] Unlike many studies in this direction which focus on obtaining better control of dispersion and distribution states through modification of the CNT surface, the current work focuses on the importance of optimal mixing of as-received CNTs through mechanical dispersion techniques.[5–7]

Commonly, ultrasonication is employed for the dispersion and stabilization of CNTs in a solvent and polymer.[8,9] Reports on the effect of ultrasonication on dispersion of CNTs have suggested several possible effects of processing conditions on the final properties of the polymer nanocomposite. For example, for epoxy with 0.5 and 1 wt% of multi-walled CNTs (MWCNTs), Gkikas et al. found a marginal increase in the nanocomposite tensile strength and tensile modulus in comparison to neat

epoxy even when the sonication time was increased from 0.5 to 4 hr.[10] It is also possible that after reaching a maximum value, nanocomposite properties decrease slowly with additional mixing until the properties approach an asymptote over time. For example, Montazeri et al. investigated the impact of sonication output powers and times on the tensile properties of MWCNT/epoxy/chopped strand mat nanocomposites.[11] They found that the tensile properties of the nanocomposite initially increased with an increase in sonication time and power; however, these properties decreased with additional time or power input, suggesting an optimal condition at which maximum mechanical properties were achieved.

While most studies have found that the CNTs agglomerates can be broken down during the earlier stages of mixing, some reports suggest CNTs can be either damaged or demixed into new agglomerate shapes and sizes during subsequent processing. For example, cavitation from the ultrasonication process has been shown to break CNTs into smaller pieces. Lu et al. reported such damage for MWCNTs, where transmission electron microscopy (TEM) observation found that ultrasonication could remove the outer walls and reduce the length of the CNTs.[12] Yu et al. also reported a change in aspect ratio of sodium dodecyl sulfate (SDS) surfactant modified single-walled CNTs in 1 wt/vol% sodium deoxycholate as a function of sonication time and power using atomic force microscopy and ultraviolet–visible (UV–vis) spectroscopy.[9] Pagani et al. have theoretically explained the two mechanisms that lead to CNT scission during ultrasonication.[13] They found from their simulations that CNT length decreases as a function of sonication time following a power law and that the exponent varies depending on the scission mechanism.[13–15] They postulated that CNT scission is due to stretching for shorter CNTs and results from a buckling mechanism for longer CNTs. Finally, Huang et al. have described in detail the criteria for dispersion and stability when using sonication.[16] They explain that the specific energy input or local energy density should be greater than the binding energy of CNT aggregates and lower than the energy required to fracture the CNTs. They then developed a model to determine the shear forces that could be generated using ultrasonication and showed an example where 10 hr of sonication led to damage of CNTs thus affecting their aspect ratio.[16]

Some researchers have also shown that excessive mixing can disrupt CNT networks originally developed during processing due to demixing and reagglomeration of the CNTs.[17,18] For example, Vural et al. have shown that linear viscoelastic properties first increase and then decrease as sonication times increase for a UV–curable CNT/poly(ethylene glycol mono acrylate) (PEGMA) nanosuspension with a CNT volume fraction of 0.003. The initial increase followed by the decrease of the linear viscoelastic moduli has been found to be consistent with corresponding optical images that show initially agglomerated CNTs in PEGMA to first become better dispersed (leading to increase of storage and loss moduli) and then begin to agglomerate (with corresponding decreases in linear viscoelastic material functions) as the sonication time further increases.[18]

The addition of small amounts of CNTs to a polymer can transform an insulating polymer into a conductive polymer nanocomposite due to the ability of CNTs to form a percolating network within the polymer.[1] Such network formation can also affect the processability and viscoelastic material functions of the nanocomposite.[3,19–22] A wide range of percolation thresholds have been reported for both electrical and rheological properties of polymer/CNT nanocomposites.[1,4] In addition, numerous studies have shown that rheological and electrical percolation thresholds strongly depend on the type of polymer, CNT aspect ratio, degree of breakdown of CNT agglomerates, and the degree of alignment and spatial distribution of the embedded CNTs.[4] Further, it has been shown that percolation thresholds exhibit a strong dependence on the processing conditions used to incorporate CNTs in the polymer.[23]

Such work highlights the importance of understanding the conditions under which networks of CNTs form and how they can be damaged or demixed. In our previous work, the importance of applying a two-stage (CNT and solvent) sonication process to obtain a better dispersion of CNTs and reproducible polymer nanocomposite properties was described.[24,25] Electrical, rheological, and mechanical characterization results suggest that once nanocomposite property enhancements reach an optimal level, further sonication leads to a decrease in the corresponding properties due to a combination of CNT damage and demixing mechanisms.

For this study, MWCNTs were dispersed in a polycaprolactone (PCL) polymer matrix using a solution processing technique. The CNTs were incorporated into dichloromethane (DCM) using a probe sonicator with different durations of sonication (15, 30, 60, and 90 min). This stage is referred to as Stage 1 sonication, during which the development of electrical conductivity of the CNT/solvent nanosuspension during sonication was monitored. Following Stage 1 CNT/solvent sonication, samples were then characterized using small-amplitude oscillatory shear, UV spectroscopy, and electron and optical microscopy. The samples were then subjected to an additional 10 min of PCL/CNT/solvent sonication using a probe ultrasonicator (referred to as Stage 2 sonication) and then dried in a vacuum oven for 4 days until all the solvent was evaporated, leaving the PCL/CNT nanocomposite. The resulting PCL/CNT nanocomposite samples were then molded and

subjected to rheological, mechanical, and electrical characterization. Using these wide-ranging characterization techniques, the optimum dispersion and distribution states of CNTs were sought, while documenting the effects of demixing and damage of CNTs on the electrical, tensile, and viscoelasticity of the polymer nanocomposite. While length scale effects are a challenge when considering polymer nanocomposites, a particular advantage of the approach used in this manuscript is the complementary analysis of the dispersion/distribution states of the MWCNT at several different length scales: TEM, high magnification optical characterization, and bulk properties (electrical and mechanical characterization). This work also leverages the shear-induced crystallization behavior of the sample, where changes in bulk rheological behavior are quite sensitive to the local MWCNT surface area available for nucleation.[24,25]

2 | EXPERIMENTAL

2.1 | Materials

The PCL used here was obtained from Scientific Polymers (CAT 1070 with molecular weight of 70,000 g/mol and solid density of 1,145 kg/m^3). DCM (Pharmaco-Aaper, reagent grade) was used as the solvent. MWCNTs obtained from Cheap Tubes Inc. of Boston, MA (density of 2,100 kg/m^3) typically exhibited outer diameters of 20–30 nm and lengths of 10–30 μm, resulting in an aspect ratio ranging from 330 to 1,500. For the studies reported here, the concentration of CNT in PCL was varied between 0.3 wt% (0.05% by volume) and 2 wt% (1.1% by volume).

CNTs typically exhibit very large aspect ratios and occupy correspondingly high hydrodynamic volumes. Consequently, CNTs overlap and aggregate at concentrations as low as 0.1 wt%.[26] Two concentration regimes can be defined on the basis of the number density and dimensions of CNTs, that is, the semidilute and the concentrated regimes. In the semidilute regime, the nanotubes cannot rotate freely without being impeded by their neighbors, whereas in the concentrated regime, the isotropic packing of the nanotubes becomes difficult. The concentrated regime for well-dispersed CNTs is generally characterized with $cL^3 >> 1$ and $cL^2d \leq 1$ (where c is the number density, d is the outer diameter, and L is the nanotube length).[27] A range of CNT concentrations, that is, volume fractions, ϕ, of 0.0015 (0.3 wt%) to 0.0044 (0.8 wt%) were used for the characterization of electrical properties of the CNT/PCL nanocomposites, while all other experimental results reported here were carried out at $\phi = 2.7 \times 10^{-3}$. At this concentration, and with CNTs where $L = 20$ μm and $d = 25$ nm, $cL^2d = 2.8$ and $cL^3 = 2{,}215$, indicating that when well distributed the CNTs would be in the concentrated regime. The development of a percolating CNT network would be expected at the concentrated regime of CNTs.

2.2 | Solution mixing of CNTs with PCL and sample preparation

Ultrasonication is a mixing technique where mechanical vibrations are transmitted through a horn tip immersed in a liquid solution. These vibrations generate ultrasonic cavitations which collapse and help to overcome the binding energy between nanotube surfaces, which leads to deaggregation of the CNTs. The sonication apparatus used here was a Misonix XL2020 ultrasonic unit.

Here, a two-stage sonication procedure was applied.[24,25] During the first stage in the mixing procedure ("Stage 1" sonication), the CNTs were sonicated and dispersed in DCM (0.05 g CNT with 50 ml of DCM) for 15, 30, 60, and 90 min. Separately, the dissolution of 9.95 g of PCL in 100 ml of DCM was carried out using a magnetic stirrer for 50 min under ambient temperature conditions. The Stage 1 CNT/DCM mixtures were then directly added to the PCL/DCM solutions, with the combined mixture (PCL/CNT/DCM) sonicated for an additional 10 min ("Stage 2" sonication). For all sonication operations, the power input was estimated to be in the range of 60–70 W. It was verified using a thermal imaging camera (Inframetrics PM290) that under these power conditions the temperature of the suspension did not rise significantly.

The resulting sonicated mixtures (i.e., after Stage 2) were vacuum dried at 50°C for 4 days until all solvent was evaporated. After complete drying (as verified with successive weight measurements), the nanocomposite samples were stored in low-density polyethylene bags in a desiccator to be used for molding and characterization as described below.

2.3 | Electrical conductivity during sonication

Electrical conductivity versus time behaviors of the Stage 1 CNT/DCM suspensions were obtained by measuring current flow using a probe built in-house with fixed area and constant gap between two electrodes. The probe was immersed into a beaker containing the CNT/DCM suspension at 15 min sonication intervals. The readings were taken after allowing the suspension to relax (no sonication) for 1 min. The electrical conductivity was determined by measuring the current flowing through the sample at a

constant voltage source of 15 V. Resistance values for each mixing condition were calculated from the inverse slope of voltage versus current for each sample, from which the electrical conductivity σ of the samples was calculated as:

$$\sigma = \frac{L}{RA}, \quad (1)$$

where R is the resistance, A is the cross-sectional area of the electrodes, and L is the gap between the two electrodes. The value of the geometry constant L/A was obtained by calibrating the setup using a standard solution for electrical conductivity (i.e., HI6033 84 μS/cm standard solution available from Hanna Instruments).

2.4 | UV–vis characterization

Spectroscopic methods can be used to quantify nanotube dispersion by correlating the amount of light absorbed by the suspension to the concentration of the nanoparticles.[28,29] Specific to our work here, UV–vis has been used to study the dispersion of MWCNT systems.[5,30–34] For example, Alafogianni et al. evaluated the dispersion quality of sonication of an aqueous solution of MWCNT and dispersive agent, finding that longer sonication time led to a higher characteristic peak in UV–vis spectra.[5] As the absolute value of the UV–vis spectra contains information about both scattering and absorption, they used liquid mode laser diffraction to measure particle sizes.[5] Similarly, Yu et al. studied the dispersion quality of sonicated MWCNTs with aqueous surfactants and found the optimal achievable dispersion of MWCNTs corresponds to maximum UV absorption of the solution.[30] A comprehensive review of spectral analysis techniques to characterize the dispersion of CNTs in aqueous suspensions is presented in the literature.[28] In this work, we have used the relative difference and confidence intervals of the spectra absorbance values to analyze the dispersion of the nanotubes.

For UV–vis spectroscopy work conducted here, 100 μl samples at the end of each Stage 1 sonication mixing procedure were placed into quartz cuvettes and further diluted by a factor of 20 using the same DCM solvent, after which the UV spectra of the samples were recorded. For background, blank quartz cuvettes were employed, and for reference, pure DCM was measured under the same conditions as the samples themselves and subtracted from the absorbance signal of the samples. For each mixing condition, UV–vis spectra for 10 samples were obtained. For the mixing index values described below, absorbance values at a specific wavelength of 500 nm were used.

2.5 | Microscopy

Microscopy coupled with image analysis is an effective method for characterizing agglomerate sizes and their distributions.[20,35–41] For TEM, a Lacey carbon-coated Copper 300 mesh grid, purchased from Ted Pella Inc (Lacey Carbon Type A, Copper (#01890)) was used. The formvar layer on the grid was removed by dipping the grid in chloroform for 10 s and allowing it to dry sufficiently in open air. Following this, a 5 μl drop of CNT/DCM suspension obtained after Stage 1 sonication was placed on the grid and allowed to dry in open air for 5 min, leaving the CNTs to be imaged on the grid. For TEM, a JEOL 1010 TEM was used.

Optical microscopy used a Nikon Eclipse E1000 microscope. Here, 2 μl drops of PCL/CNT/DCM obtained following Stage 2 sonication were placed on glass slides that were then covered with glass cover slips. Optical images were obtained at a magnification of ×20 and recorded using a digital camera at room temperature.

ImageJ software was used for the analysis of microscopy images. The images were digitized to 8 bit and then subjected to binarization.[19,35,36] Binarization was carried out using the Triangle Thresholding algorithm of ImageJ.[36] Using this approach, the diameters of CNT aggregates and the area fractions of the aggregates were found.

2.6 | Rheological characterization

Linear viscoelastic properties of the nanocomposite samples were found via small-amplitude oscillatory shear experiments using an Advanced Rheometric Expansion System from TA Instruments. The rheometer was equipped with a force rebalance transducer (2K-FRTN1) and an environmental chamber which maintains a constant temperature within ±0.1°C. For linear viscoelastic property characterization, the samples were first melted in the rheometer at a temperature of 80°C for 5 min. A 1 mm gap was then set between two 25 mm diameter parallel plates and the excess material trimmed. The environmental chamber was then reclosed and allowed to reequilibrate at 80°C post-trimming for at least 5 min prior to testing.

The dynamic viscoelastic properties were characterized as a function of frequency between 0.1 and 100 rad/s. Characterization of the linear viscoelastic response of the CNT/PCL nanocomposites over a range of frequencies (and hence time scales) provides a broad description of their viscoelastic responses. In general, at relatively small characteristic deformation times (high frequencies) the elastic response is accentuated while at longer characteristic times (low frequencies), the viscous flow

behavior is accentuated. It was determined that the samples were in the linear viscoelastic regime for strain amplitudes that were ≤1%. The frequency sweeps were carried out at a strain amplitude of 1% and at 80°C.

It has been shown that the shear-induced crystallization behavior of polymer nanocomposites can be quite sensitive to the state of dispersion of CNTs within a semicrystalline polymer.[24,25] During shear-induced crystallization, the nanoparticles can act as heterogeneous nuclei and alter the crystallinity development for nanocomposites of CNTs dispersed into semicrystalline binders.[21,42,43] The shear-induced crystallization tests were also conducted using the rheometer. The steps of loading and equilibrating the samples at 80°C were similar to the procedures used for the characterization of dynamic properties, as described above.

The crystallization temperatures of the pure PCL and the 0.5 wt% PCL/CNT nanocomposite were found to be 28 and 38°C, respectively.[25] Upon waiting approximately 2 min following thermal equilibration at 80°C, the shear-induced crystallization experiments were started by cooling the samples to the target temperature of 55°C at a rate of 15°C/min. Dynamic viscoelastic properties were then collected at 1% strain amplitude and 1 rad/s as a function of time. Changes in the viscoelastic properties as a function of time are associated with the shear-induced crystallization behavior of the PCL/CNT nanocomposite. Three samples were tested for each condition.

2.7 | Mechanical properties

To evaluate the effects of the CNT dispersion and distribution states on mechanical properties, tensile properties of the PCL and 0.5 wt% PCL/CNT nanocomposite samples were characterized. Storage moduli at room temperature were characterized using an INSTRU-MET floor model Instron with Testworks material software, with tests performed according to ASTM D882. Rectangular samples with a thickness of 0.87 mm, width of 21.8 mm, and a gage length of approximately 25 mm were used for the tensile tests. The specimens were tested in displacement control mode at a crosshead speed of 0.25 mm/min. For each mixing condition, three samples were tested.

2.8 | Electrical characterization

For electrical characterization, PCL/CNT nanocomposite samples were subjected to different Stage 1 sonication durations followed by 10 min of Stage 2 sonication. Earlier work had shown that this procedure provides an effective processing method for the PCL/CNT suspension samples.[24,25] PCL/CNT suspensions that were subjected to Stage 2 mixing and subsequent drying were compression molded using a Carver compression molder. Six rounded-edge rectangular samples approximately 10 mm in length, 6.5 mm in width, and 1.2 mm in thickness were molded using an aluminum shim under a pressure of 138 MPa at 100°C for 5 min. Samples were coated with silver paint on the edges to minimize the contact resistance with the electrodes. These samples were used to measure current as a function of varying voltage from 1 to 30 V applied in steps of 0.5 V using a Keithley 2636B dual channel source meter which was calibrated using a known source of resistance.

2.9 | Degree of distributive mixing: mixing index

A quantitative description of the mixing quality of a given mixture can be obtained by determining the concentration distributions of the minor phase at a given scale of examination.[44–49] A relatively low mixing index (MI) value represents poor distributive mixing efficacy while larger MI values represent better homogeneity. The formulae that are used in mixing index calculation have been presented in our previous work.[24,25]

Briefly, if one makes N measurements of the concentration c_i of the minor component, then the mean concentration $\bar{c}$ can be written as:

$$\bar{c} = \frac{1}{N}\sum_{i=1}^{N} c_i. \tag{2}$$

The variance s^2 of the individual concentration c_i measurements provides a means to quantitatively assess the degree of mixedness and can be written as:

$$s^2 = \frac{1}{(N-1)}\sum_{i=1}^{N} (c_i - \bar{c})^2. \tag{3}$$

A small variance indicates that the concentrations c_i are close to the mean concentration $\bar{c}$ and thus a relatively homogeneous mixture has been achieved. On the other hand, the maximum variance s_0^2 corresponds to the complete segregation of the minor and major components such that

$$s_0^2 = \bar{c}(1-\bar{c}). \tag{4}$$

Normalizing the standard deviation s with respect to its maximum value obtained for the segregated state s_0, the mixing index MI is defined as:

$$MI = 1 - s/s_0. \quad (5)$$

3 | RESULTS

Sonication is a powerful technique to process polymer nanocomposites and has been studied in detail to develop processing techniques that aid in better dispersion and distribution of CNTs in the polymer matrix. In the current work, the focus is to understand the effects of longer than optimal ultrasonication times on the dispersion and distribution states of the CNTs and the resulting electrical and rheological properties of the nanocomposite.

3.1 | Electrical conductivity during sonication

Electrical conductivity of the Stage 1 CNT/DCM solution is obtained by measuring the current flow through the sample subjected to a voltage source of 15 V. The current measured is then converted to conductivity using Equation (1) and plotted in Figure 1. It is observed in Figure 1 that electrical conductivity of the CNT/DCM suspension first increases as the Stage 1 sonication time increases from 15 to 30 min, and then the conductivity decreases as the sonication time is further increased.

As the CNTs are exfoliated from their bundled states during sonication they undergo deformation, bending, and buckling.[22] Furthermore, the exfoliated CNTs begin to interact with their neighbors and start to form strained network configurations. The stability of these strained network configurations is driven by the competition between the attractive van der Waals forces which are driving the CNT interactions and the elastic energies of the bent/deformed nanotubes.[16] The enhanced electrical conductivity during the earlier sonication times is associated with the development of a CNT network by CNTs that have deagglomerated and are now distributed within the solution, while decreases in the conductivity for longer durations of sonication are attributed to the disruption of the CNT network caused by either demixing or damage of the CNTs. It is clear that the measurement of the electrical conductivity of the CNT/solvent suspensions during mixing is an effective method for the monitoring of the efficacy of the mixing process during sonication.

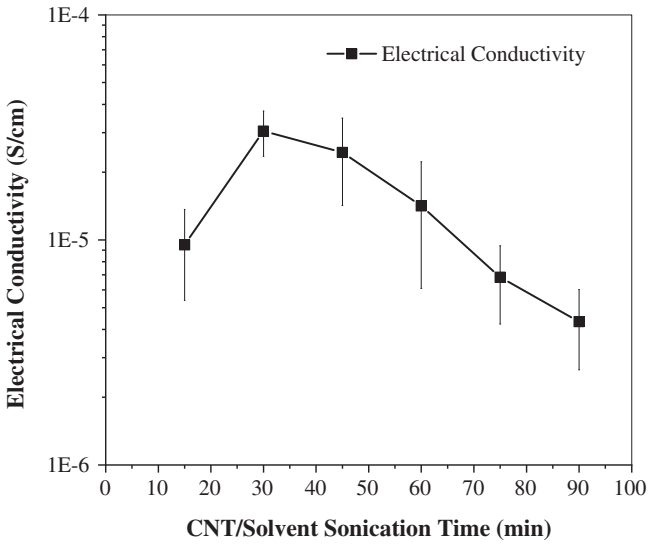

FIGURE 1 Electrical conductivity of Stage 1 carbon nanotube/dichloromethane (CNT/DCM) suspensions (average values obtained for three samples)

3.2 | UV–vis characterization

UV–vis spectroscopy, based on quantifying the absorption of light in the UV–vis spectrum, is applicable to any type of suspension and is one of the most straightforward techniques for characterizing the dispersion of the CNTs.[5,29] While individual CNTs absorb light in UV–vis region, CNT bundles do not, and thus as the CNTs are better dispersed the suspension will absorb more light, suggesting the use of UV–vis as an indicator of dispersion quality.[28,29,31] Here, UV–vis spectra were obtained for 10 samples for each Stage 1 sonication time, with the average absorbance values and the 95% confidence intervals for each wavelength plotted in Figure 2. We attribute small fluctuations in the curves to sample concentration effects and sample-to-sample variation.

As shown in Figure 2, all samples have a characteristic peak in their UV–vis spectrum at a wavelength of approximately 250 nm in agreement with the literature.[29] It is further observed that increasing the sonication time for the suspension from 15 to 30 min leads to an increasing amount of unbundled CNTs, which results in an increase in absorbance values. However, for a further increase in the sonication time to 60 or 90 min, the absorbance values decrease indicating that the number of individual CNTs absorbing the light has been reduced. This would indicate that beyond the optimal sonication time, the additional sonication energy results in partial reagglomeration or bundling of the CNTs in this particular system.

To further characterize the distribution of CNTs using UV–vis spectroscopy, the absorbance values at 500 nm were examined as reported in previous studies.[31] Figure 3 shows the absorbance values at 500 nm from each of the 10 samples for each mixing condition. From Figure 3, it was found that for suspensions that were

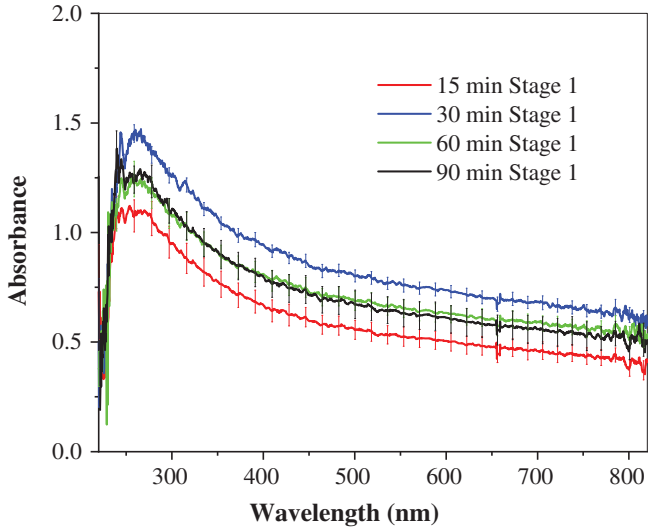

FIGURE 2 Average ultraviolet–visible (UV–vis) absorption spectra and 95% confidence intervals as a function of Stage 1 sonication times. Each line represents the average of 10 samples of 100 μl of carbon nanotube/dichloromethane (CNT/DCM) diluted by a factor of 20 [Color figure can be viewed at wileyonlinelibrary.com]

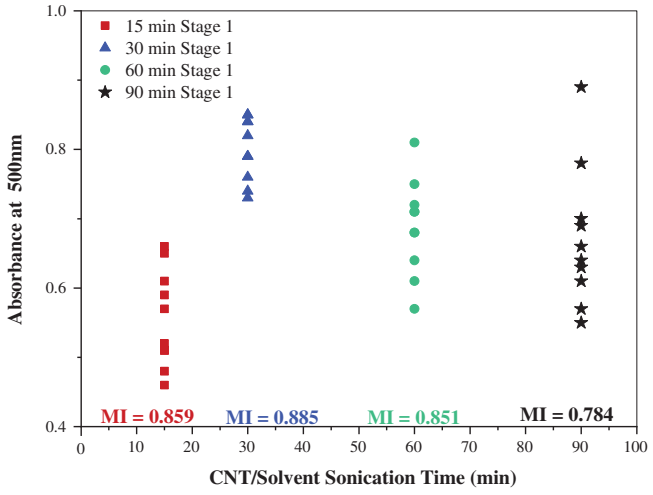

FIGURE 3 Ultraviolet–visible (UV–vis) absorbance values at 500 nm for carbon nanotube (CNT)/solvent samples taken after different durations of Stage 1 sonication and corresponding mixing indices [Color figure can be viewed at wileyonlinelibrary.com]

subjected to 15 min of Stage 1 sonication, the absorbance values at 500 nm range from 0.45 to 0.65, while for 30 min of Stage 1 sonication, the absorbance values range from 0.75 to 0.85. Samples subjected to 60 min of Stage 1 sonication have absorbance values that range from 0.58 to 0.82, while finally for samples subjected to 90 min of Stage 1 sonication the absorbance values range from 0.55 to 0.9. A tighter spread in the range of absorbance values indicates better distribution of the dispersed CNTs within the samples.

In addition, also shown in Figure 3 are mixing indices based on the absorbance values at a wavelength of 500 nm for each mixing condition. These values were determined using Equation (5). It is noted that the mixing index values increased from 0.859 (for a Stage 1 sonication time of 15 min) to 0.885 for a Stage 1 sonication time of 30 min. However, as the Stage 1 sonication time is further increased to 60 or 90 min, the mixing index values reduce to 0.85 and then 0.78 indicating that there is greater variation from the mean absorbance for longer sonication times. This suggests that the homogeneity of the distribution of CNTs in the CNT/solvent suspensions improves during the first 30 min of sonication but then deteriorates at longer sonication times.

3.3 | Morphological characterization

TEM was used to obtain direct images of the CNTs after Stage 1 sonication as described in the experimental section. Figure 4 shows images of CNTs that were sonicated for 15, 30, 60, and 90 min, respectively, at ×20,000 magnification.

For 15 min of sonication, the CNTs appear to be starting to become unentangled with longer lengths observed for the CNTs, while the CNTs subjected to 30 min of sonication appear to be well distributed and form a loosely packed network while their lengths remain similar. On the other hand, it is observed in Figure 4c,d that CNTs subjected to 60 or 90 min of Stage 1 sonication seem to have a reduction in their lengths (highlighted by yellow arrows) along with some local aggregation in comparison to samples subjected to 15 and 30 min of Stage 1 sonication.

It is also observed in Figure 4c,d that the CNTs sonicated for longer durations tend to bend and buckle (highlighted by red arrows). Such bending and buckling are expected on the basis of the theoretical calculations of Pagani et al.[13] Different models have been presented in the literature to explain the fracture or breaking of CNTs during ultrasonication. For example, Huang et al. proposed a model that defined a filament fracture resistance parameter as $0.5 \times \sigma \times (d/L)^2 < \sigma_{\text{sonication}}$, where σ is the tensile strength of the CNT. For the current system using an average d of 25 nm and L of 10 μm, we get the fracture resistance parameter to vary between 32 and 312 kPa for tensile strengths of 10–100 GPa as reported in the literature.[16,50,51] In addition, Huang et al. reported that the localized shear stress imparted in the vicinity of an exploding cavitation bubble in a low viscosity system is on the order of 100 MPa.[16] The amount of energy provided by ultrasonication far exceeds this value and is thus able to break the CNTs. However, the fracture resistance parameter is dependent on the length of the nanotubes

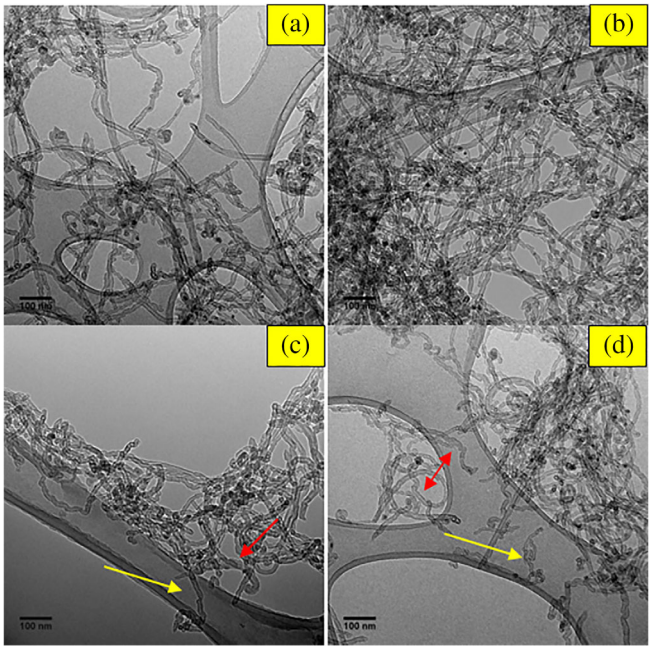

FIGURE 4 Transmission electron microscopy images of carbon nanotubes subjected to different Stage 1 sonication times: (a) 15, (b) 30, (c) 60, and (d) 90 min. Images taken at ×20,000 and scale bars represent 100 nm [Color figure can be viewed at wileyonlinelibrary.com]

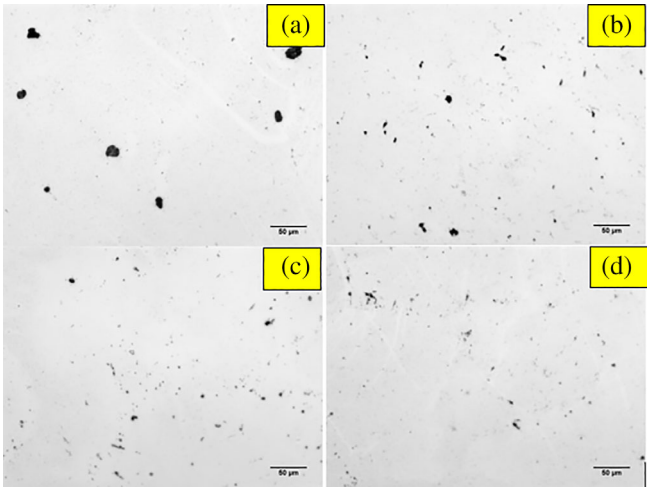

FIGURE 5 Optical images of carbon nanotubes subjected to different Stage 1 sonication times: (a) 15, (b) 30, (c) 60, and (d) 90 min followed by 10 min of Stage 2 sonication. Images taken at ×20 and scale bars represent 50 μm [Color figure can be viewed at wileyonlinelibrary.com]

and will not affect nanotubes shorter than a critical length which may buckle and bend during sonication.[13,16]

As the TEM images represent a very small fraction of the sample solution after Stage 1 sonication, optical images have also been taken and used with image analysis to characterize the diameters and the area fraction occupied by the CNT agglomerates after Stage 2 sonication.

While TEM images were obtained directly after Stage 1 sonication, we now investigate the resulting nanocomposites after subjecting the samples to a Stage 2 sonication time of 10 min. Figure 5 shows representative optical images of PCL/CNT samples subjected to different durations of Stage 1 sonication (followed by 10 min of Stage 2 sonication). It can be observed that as Stage 1 sonication time increases, the size of the CNT agglomerates decreases, with changes in the sizes of the agglomerates less discernible in samples subjected to longer sonication duration.

For each Stage 1 sonication time, 24 images similar to those shown in Figure 5 were used to analyze the distribution of the areas of the CNT agglomerates. Each of the images was analyzed using ImageJ software, with thresholding using the Triangle algorithm available within the software.

Figure 6a shows the distributions of the CNT agglomerate surface areas for different Stage 1 processed samples. Assuming that the surface areas of the agglomerates would be proportional to the volumes and hence the sizes of the agglomerates, Figure 6a suggests that Stage 1 sonication reduces the size of the agglomerates. It is observed that the number of agglomerates with surface areas less than 1–10 μm^2 increases as the Stage 1 sonication time is increased. Thus, the Stage 1 sonication appears to play a significant role in CNT disentanglement which ultimately enables better distribution within the PCL matrix polymer.

Figure 6b shows the average surface areas of the CNT agglomerates found using optical microscopy and image analysis. The average surface areas of the CNT agglomerates reduce from nearly 4.5 to 3.1 μm^2 for samples subjected to Stage 1 sonication durations of 15 and 30 min, respectively. On the other hand, it is observed that the average area of the CNT agglomerates only slightly reduces from 3.1 μm^2 to approximately 2.6 μm^2 as the Stage 1 sonication duration is further increased from 30 to 90 min, indicating that continued Stage 1 sonication becomes less effective in reducing the agglomerate size once a critical sonication time (for a given sonication power) has been reached.

The distributions of the area fractions of the CNT agglomerates as a function of the sonication time are shown in Figure 7. At each sonication time, 24 images were collected and analyzed and the corresponding mixing index values were computed based on Equation (5). It is observed that the mixing index first increases from 15 to 30 min of mixing but decreases as the sonication time is increased from 30 to 60 and 90 min of Stage 1 sonication. This suggests that although there is

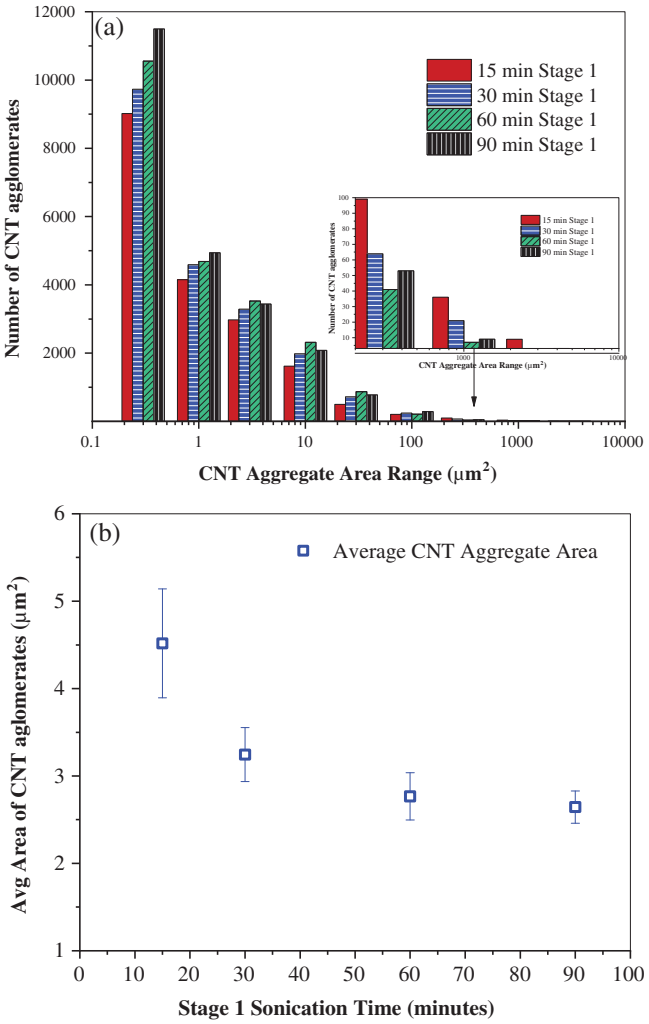

FIGURE 6 (a) Distribution of carbon nanotube (CNT) aggregate area. (b) Average area of the CNT agglomerates from optical images of polycaprolactone (PCL)/CNT samples subjected to different Stage 1 sonication times followed by 10 min of Stage 2 sonication [Color figure can be viewed at wileyonlinelibrary.com]

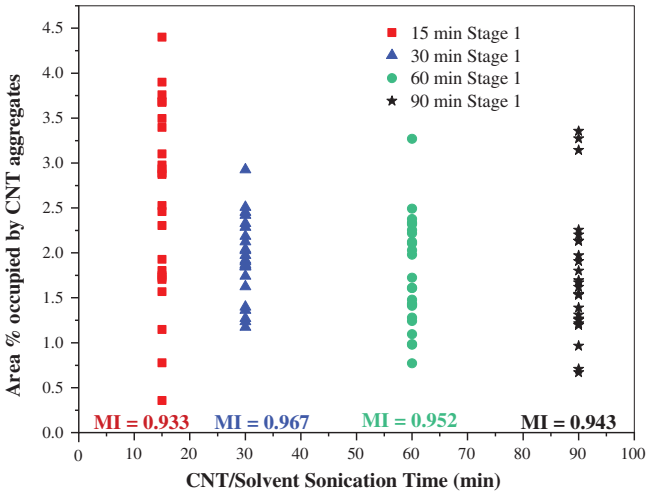

FIGURE 7 Mixing index calculated from the area percentage occupied by carbon nanotube (CNT) aggregates of polycaprolactone (PCL)/CNT samples subjected to different Stage 1 times and 10 min of Stage 2 sonication [Color figure can be viewed at wileyonlinelibrary.com]

a monotonic decrease of the agglomerate sizes with increasing sonication time (Figure 6b) the homogeneity of the spatial distribution of the agglomerates only improves going from 15 to 30 min of sonication. This is followed by the deterioration of the homogeneity of the spatial distribution of the CNTs within the solvent with the increasing of the Stage 1 sonication times beyond 30 min.

TEM images suggest the reduction of CNT lengths (and hence CNT aspect ratios) with increasing Stage 1 sonication times. The results from UV–vis spectroscopy and optical microscopy coupled with image analysis suggest that the highest degree of spatial homogeneity is obtained at 30 min of Stage 1 sonication. Furthermore, optical microscopy suggests that the sizes of the CNT agglomerates are gradually/asymptotically reduced while there is an increase in the variance of the CNT agglomerate sizes. The findings from optical image may simultaneously promote a complex coupling of CNT damage and demixing mechanisms.

3.4 | Rheological characterization

Linear viscoelastic properties were characterized for the PCL/CNT suspensions at 80°C at 1% strain amplitude. Figure 8 shows the log–log plot of the storage modulus response of PCL incorporated with 0.5 wt% CNT for different Stage 1 sonication times (all samples were subjected to 10 min of Stage 2 sonication). Also shown in the figure are the 95% confidence interval bars. Figure 8 shows that as the Stage 1 sonication time is increased from 15 to 30 min, the storage modulus also increases over the frequency range of 1–100 rad/s, with larger differences noted at lower frequencies. Greater values of storage modulus are indicative of a greater elasticity. This indicates that for the PCL/CNT samples subjected to 30 min of Stage 1 sonication, the CNTs were able to form an effective particle-to-particle network which increased the elasticity of the nanosuspension in comparison to those sonicated at lower sonication times.

However, when the Stage 1 sonication time is increased from 30 to 60 or 90 min, the storage modulus of the corresponding PCL/CNT samples decrease to values that are lower than the storage modulus for the 30 min Stage 1 sonicated samples. Overall, these findings suggest that the CNT network in the PCL matrix initially improves for samples subjected to 30 min of Stage

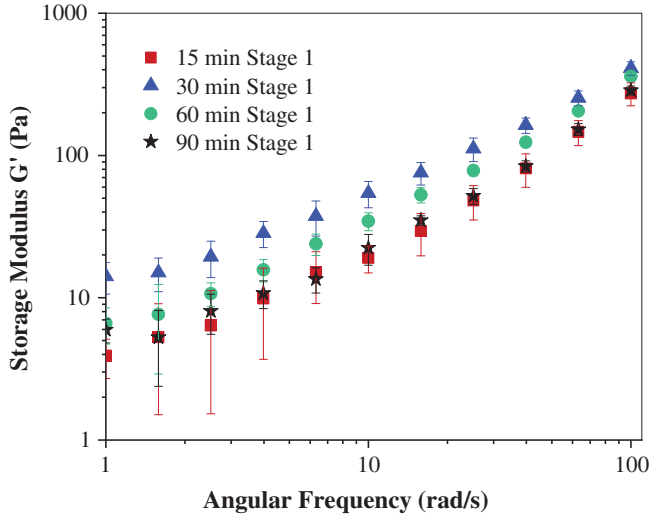

FIGURE 8 Storage modulus as a function of frequency for polycaprolactone/carbon nanotube samples at 80°C and 1% strain amplitude for different Stage 1 sonication times [Color figure can be viewed at wileyonlinelibrary.com]

1 sonication. However, it appears that for samples subjected to 60 or 90 min of Stage 1 sonication, the network formation and distribution of the CNT aggregates in the samples have been negatively affected. These results follow the same trend observed with the UV characterization of the Stage 1 CNT/solvent state as shown in Figure 2. These results also suggest that the relative dispersion and distribution states of the CNTs obtained after sonication of CNT/solvent is maintained during and after the Stage 2 sonication step.

3.5 | Shear-induced crystallization studies

Melts of semicrystalline polymers undergo accelerated crystallization under flow and deformation. CNTs can act as heterogeneous nucleating agents and accelerate the rate of crystallization under flow; they may also impact the crystallite morphology which results from shear-induced crystallization in comparison to crystallization under quiescent conditions.[42,43] Thus, the dispersion states and the sizes of the CNT agglomerates, and the associated changes in the surface areas of CNTs available for nucleation of the crystallites to occur, should play significant roles during the development of shear-induced crystallization behavior.[24,25]

A semilog plot of the shear-induced crystallization behavior of PCL/CNT nanocomposite samples with 0.5 wt% loading of CNTs is shown in Figure 9. The 95% confidence interval bars are also shown in Figure 9. The

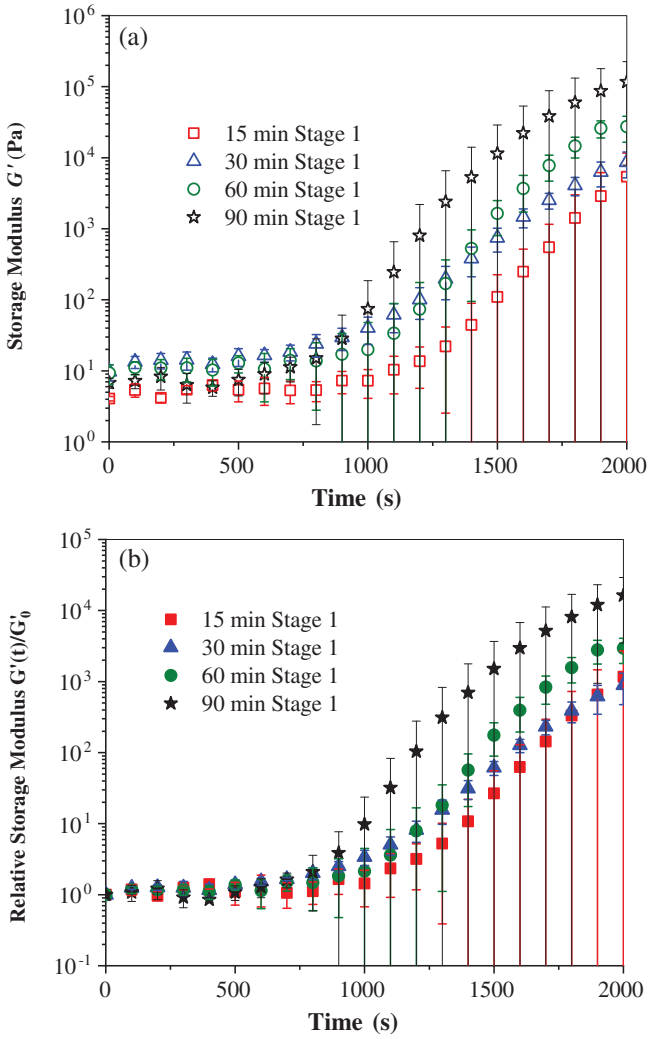

FIGURE 9 Semilog plots of (a) average storage modulus G' and (b) average relative storage modulus ($G'(t)/G'(t=0)$) as a function of time for nanocomposite samples undergoing shear-induced crystallization. Three samples for each condition were tested at 1% strain amplitude and 1 rad/s at 55°C. All samples were subjected to 10 min of Stage 2 sonication [Color figure can be viewed at wileyonlinelibrary.com]

experiments were carried out via time scans of the linear viscoelastic material functions at 55°C with a constant strain amplitude of 1% and a constant frequency of 1 rad/s. The temperature of the experiment, 55°C, is above the quiescent crystallization temperature of the samples (as indicated using differential scanning calorimetry at cooling rates of 10°C/min, crystallization occurs around 28°C for pure PCL and around 38°C for the PCL/CNT nanocomposite).

It is observed in Figure 9a that for times less than 1,000 s (prior to the induction time where the storage modulus begins to increase), the 30 min Stage 1 PCL/CNT samples exhibit higher storage modulus values in

comparison to PCL/CNT samples for which the CNT/solvent was sonicated for 15, 60, or 90 min. These results also match the trend in linear viscoelastic materials functions in the melt condition as shown previously in Figure 8.

Figure 9b shows that after an initial period of a few hundreds of seconds, the relative storage modulus of the PCL/CNT samples (storage modulus of the nanosuspension over the storage modulus of the PCL binder at the same frequency) exhibit monotonic increases with time. Since in our previous work we have shown that pure PCL control samples do not undergo shear-induced crystallization over the time span of 12,000 s under these conditions,[24,25] the increases in the dynamic properties with time during oscillatory shearing are attributed to shear-induced crystallization promoted by the presence of the CNTs. It is also observed that the nanosuspension samples subjected to longer CNT/solvent sonication times exhibit faster shear-induced crystallization in comparison to those samples that were subjected to shorter sonication times. Our previous work suggests that shear-induced crystallization is very sensitive to different dispersion states arising from different sized agglomerates and can thus differentiate differences in dispersion states due to reagglomeration.[24,25]

From Figure 9, it could be hypothesized that as the sonication time of CNT/solvent increases, and as the CNT aggregates are being broken down to a greater extent with increasing sonication time (Figure 6b), greater CNT surface areas become available for nucleation. With the availability of greater surface area for nucleation, the crystallization rate becomes faster which is reflected in the corresponding rate of increases of the dynamic properties. Shorter induction times are observed for PCL/CNT samples with longer Stage 1 sonication times. The variation of the confidence intervals of the dynamic properties with increasing sonication time should also be noted. The breadths of the confidence intervals increase with increasing sonication time, presumably due to the deterioration of spatial homogeneity of the CNTs observed in the UV absorbance at 500 nm data (Figure 3) and area percentage occupied by CNT aggregates from optical images (Figure 7).

3.6 | Mechanical properties

Figure 10 shows the tensile modulus of the PCL/CNT nanocomposites as a function of the Stage 1 sonication time. The tensile modulus of PCL/CNT samples subjected to 30 min of Stage 1 sonication is greater than those of PCL/CNT samples subjected to 15, 60, or 90 min of Stage 1 sonication. This trend is consistent with the variation of the storage modulus at 80°C as a function of the sonication time (see Figure 8) and confirms that the ultimate

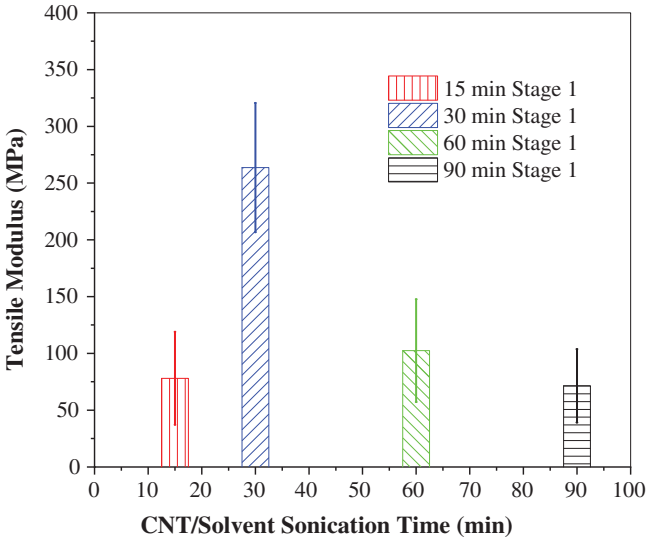

FIGURE 10 Tensile modulus of polycaprolactone/carbon nanotube (PCL/CNT) samples with 0.5 wt% CNT subjected to different Stage 1 sonication times [Color figure can be viewed at wileyonlinelibrary.com]

properties of the PCL/CNT nanocomposite initially increase as the dispersion and distribution of CNTs improve in the polymer, ultimately reaching optimal states beyond which the elastic modulus and the tensile modulus decrease with increasing sonication time, consistent with the optimum values of mixing indices observed at 30 min of sonication time (see Figures 3 and 7).

3.7 | Electrical conductivity characterization of the PCL/CNT nanocomposite

The electrical conductivity of PCL/CNT nanocomposites with different Stage 1 sonication times is presented in Figure 11. The electrical conductivity of the PCL/CNT samples processed with 30 min of Stage 1 sonication was higher than the PCL/CNT samples subjected to 15, 60, or 90 min of CNT/solvent sonication. This again confirms that the CNT network formation for the samples, which initially improves going from 15 to 30 min of CNT/solvent sonication, deteriorates as the CNT/solvent sonication time is further increased beyond 30 min. This suggests that the additional sonication has led to "demixing" associated with overmixing at these longer sonication times.

It is observed that the electrical conductivity values of PCL/CNT nanocomposites with 0.5 wt% CNT measured here are in the 10^{-7}–10^{-5} S/cm range. This range is consistent with the reported electrical properties for PCL nanocomposites with 0.5 wt% CNT loading from the literature. This range of values is associated with the different

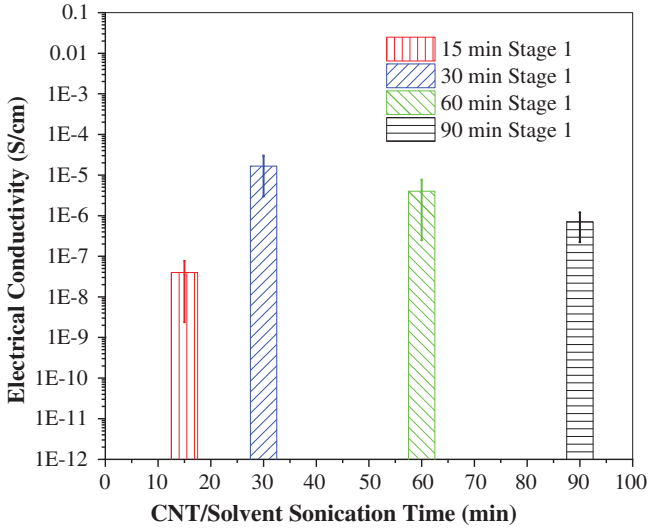

FIGURE 11 Electrical conductivity of polycaprolactone/carbon nanotube (PCL/CNT) samples with 0.5 wt% CNT loading at room temperature. Three samples were tested at each condition [Color figure can be viewed at wileyonlinelibrary.com]

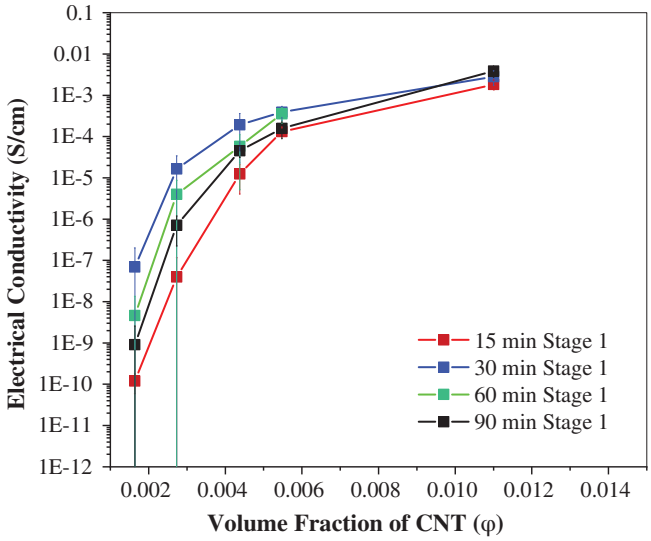

FIGURE 12 Average electrical conductivity of polycaprolactone/carbon nanotube (PCL/CNT) samples with different concentrations of CNTs subjected to different Stage 1 sonication times (six samples per test condition) [Color figure can be viewed at wileyonlinelibrary.com]

states of distributive and dispersive mixing, the agglomerate sizes, the CNT aspect ratios, and the CNT network formation which all depend on the dynamics of the mixing conditions.

The same electrical characterization procedure was repeated for samples with different CNT concentrations to understand the percolation threshold for the PCL/CNT nanocomposite samples. As shown in Figure 12, for CNT concentrations of 0.0015 volume fraction (0.3 wt%) and 0.0044 volume fraction (0.8 wt%), the samples follow a similar trend in the electrical conductivity behavior as a function of the Stage 1 mixing time as the 0.0027 volume fraction (0.5 wt%) CNT samples described in Figure 11. It is also observed that as the concentration is increased to 0.0055 volume fraction (1 wt%) or 0.010 volume fraction (2 wt%) of CNTs, the different Stage 1 mixing times do not show any appreciable difference in the electrical conductivity. Thus greater sensitivities (greater gains) in electrical conductivity to different mixing conditions are observed for samples with lower concentrations of CNTs in the PCL/CNT nanocomposite system. Based on Figure 12, for nanocomposites with lower concentrations of CNTs, that is, for PCL/CNT samples with 0.0015 volume fraction (0.3 wt%) CNTs, the electrical conductivity shifts from insulating (10^{-10} S/cm) at 15 min of Stage 1 sonication to conducting (10^{-7} S/cm) for samples subjected to 30 min of Stage 1 sonication.

It has been hypothesized that near the CNT percolation concentration ϕ_c, the DC electrical conductivity of the composite follows the relation

TABLE 1 Percolation threshold values obtained for PCL/CNT samples as a function of Stage 1 sonication time (all samples underwent Stage 2 sonication for 10 min)

Stage 1 sonication time (min)	Percolation threshold concentration (φ_c)	Constant (C)
15	0.00268	18.52
30	0.00158	32.30
60	0.00234	33.83
90	0.00258	35.83

Abbreviations: CNT, carbon nanotube; PCL, polycaprolactone.

$$\sigma_{DC} = C(\phi - \phi_c)^t, \tag{6}$$

where ϕ is the concentration of CNTs added and C is a constant which is fit to the experimental data.[20,52] Generally, the exponent t is assumed to only be a function of the dimension of the percolation system.[53] The value of t lies between 1.33 for a two-dimensional system and 2.05 for a three-dimensional system.[52–54] Assuming here a three-dimensional system with $t = 2.05$, the data in Figure 12 were curve fit to Equation (6) such that the electrical percolation threshold concentrations for different mixing conditions were determined as shown in Table 1. The lowest value for the percolation threshold occurs at 30 min of Stage 1 sonication time, with even longer Stage 1 sonication times resulting in larger values of the percolation threshold, which is attributed to the documented poorer distribution of the CNTs within the PCL binder.

Li et al. fabricated epoxy nanocomposites using various techniques to achieve different states of CNT dispersion and characterized these samples using electrical conductivity.[23] To characterize the resulting electrical percolation thresholds, they developed a theoretical model based on the concept of improved interparticle distance, where CNTs could be either entangled in agglomerates or isolated as individual CNTs, such that[23]

$$\varphi_c = \frac{\xi\varepsilon\pi}{6} + \frac{(1-\xi)27\pi d^2}{4l^2}, \quad (7)$$

where ε is the localized volume content of the CNTs in an agglomerate (describing how tight the entanglement is) and ξ is the volume fraction of the agglomerated CNTs within the binder. The parameter ε can have values between the filler volume fraction and 1, where higher values of ε indicate poorer dispersion. On the other hand, ξ can have values between 0 and 1, where 0 indicates no agglomeration and 1 indicates all the filler volume is agglomerated. Based on their model and corresponding analysis of experimental data, Li et al. found that the aspect ratio would play an important role in the percolation threshold.[23]

Based on Equation (7), the percolation threshold volume fractions can be plotted as a function of aspect ratio as shown in Figure 13. Also shown in the figure are the experimental percolation values determined for the different Stage 1 sonication times reported in Table 1. The experimental percolation threshold values have been represented as a series of symbols over a range of aspect ratios based qualitatively on evidence of the shortening of CNT length based on the characterization results presented above. In Figure 13, the curves are based on one set of parameter values ε and ξ which appear to fit the experimental percolation threshold range. It is clear from Figure 13 that the effect of a reduction in CNT aspect ratio on the percolation threshold would only become noticeable once the aspect ratio is less than 200–400.

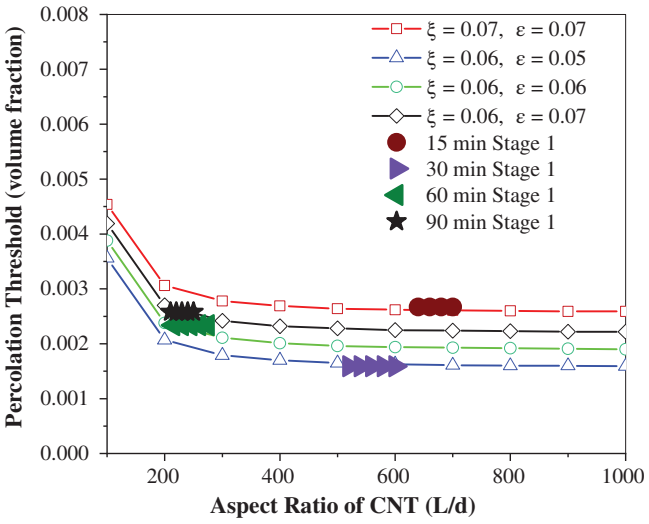

FIGURE 13 Effect of dispersion parameters on percolation threshold of polycaprolactone/carbon nanotube (PCL/CNT) samples based on the model developed by Li et al.[23] Symbols denote the percolation thresholds calculated from the current study for different Stage 1 sonication times [Color figure can be viewed at wileyonlinelibrary.com]

4 | DISCUSSION

A two-stage sonication/mixing process has been applied to distribute (to achieve spatial homogeneity) and disperse (to reduce the agglomerate sizes) CNTs first in a DCM solvent and then in a PCL binder followed by the removal of the solvent. Various methods were applied to show that there are optimal mixing/sonication conditions for CNT/solvent nanosuspensions. The use of an electrical conductivity probe allowed the monitoring of the electrical conductivity during Stage 1 sonication. It was observed that the CNT/solvent nanosuspension exhibited a maximum conductivity at 30 min of sonication. This suggested that the CNTs could be well distributed and dispersed at 30 min of sonication but that the distribution and dispersion states deteriorated with increasing sonication time. Other analysis methods including TEM, UV–vis absorbance, and optical microscopy supported this conclusion. For example, in UV–vis spectroscopy, the absorbance first increased as the Stage 1 sonication time was increased from 15 to 30 min and then decreased with longer (60 and 90 min) sonication time (Figure 3). Because absorbance is directly related to the concentration of individual CNTs, the UV–vis characterization results support the activation of a demixing mechanism for sonication durations greater than 30 min.

Furthermore, TEM images (shown in Figure 4) provide direct evidence that both CNT length scission and local reagglomeration also occur at sonication times longer than the optimal (30 min) identified with electrical conductivity and UV–vis spectroscopy of CNT/solvent nanosuspensions. This interpretation would also be consistent with reports from the literature.[5,9]

Effective nanocomposite properties such as tensile modulus (Figure 10) and electrical conductivity (Figure 11) demonstrated optimal properties at 30 min of Stage 1 sonication, with properties deceasing as the sonication time was further increased. However, the CNT aggregate sizes in PCL decreased monotonically with increasing Stage 1 sonication time. In addition, the induction times for shear-induced crystallization were also

smallest for 90 min of Stage 1 sonication and increased monotonically with decreasing Stage 1 sonication time.

Based on the optical image analysis of the PCL/CNT samples shown in Figure 6, it is observed that the average area of the CNT agglomerates reduces asymptotically as the Stage 1 sonication time increases. However, if only the CNT damage mechanism was present during the sonication process, then the size of the CNT agglomerates would continue to decrease and the UV–vis absorption spectra would continue to increase as a function of sonication time. In addition, if only the CNT damage mechanism were to occur, then the distribution of the CNTs would increase and reach a plateau state beyond which the distribution of the CNTs would not be significantly affected with excessive sonication times, which is not consistent with the results obtained in this work.

The mixing index analysis of the average area fraction of CNTs in PCL (see Figure 7) shows that the distribution of the CNT agglomerates first increases, then reaches a maximum value, and then decreases as the Stage 1 sonication time further increases. A similar conclusion was observed from the shear-induced crystallization results, where it was observed that the induction time reduces as Stage 1 sonication time increases, indicating that more CNT surface area becomes available for nucleation as the sonication time increases. The variation in the dynamic properties for the shear-induced crystallization behavior and the decrease in the mixing index values support the reagglomeration mechanism, and that the distribution of CNTs is negatively affected with excessive Stage 1 sonication. However, if only reagglomeration of CNTs were to occur after excessive sonication, the CNT agglomerates would first decrease in size with increasing sonication, and then increase in size for excessive sonication, which would be reflected in the corresponding optical image analysis, TEM images, and shear-induced crystallization behavior. However, as this is not the case, we conclude that both damage and demixing mechanisms occur concomitantly.

Similarly, the results obtained from the dynamic melt properties and the solid state electrical conductivity of the PCL/CNT nanocomposite samples suggest the initial formation of a (partial/weak) CNT network with the increase in dispersion and distribution of the CNTs with 30 min of Stage 1 sonication time, with further sonication leading to a deterioration of the network, a decrease in electrical conductivity, and a reduction in the storage modulus. This also results in the peak mechanical properties observed for 30 min of Stage 1 sonication time shown in Figure 10. Thus, based on the inferences drawn from these different characterization techniques, it can be postulated that the CNT agglomerates begin to break down and distribute through the solvent volume with

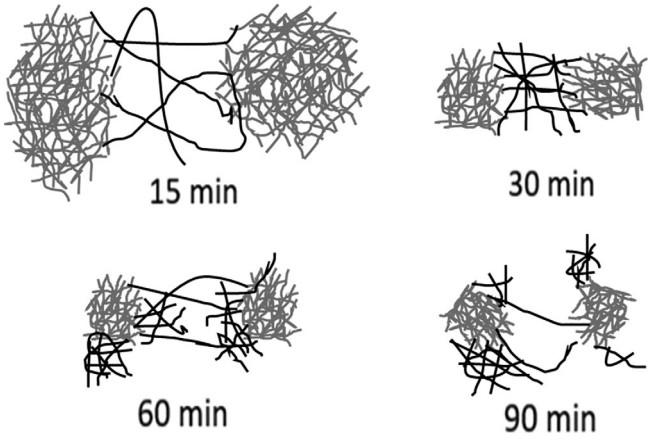

FIGURE 14 Schematic of the carbon nanotube dispersion and distribution in the solvent as the Stage 1 sonication time is increased from 15 to 90 min

15 min of Stage 1 sonication, and that the distribution reaches optimal conditions at 30 min of sonication time. However, a further increase in Stage 1 sonication duration up to 60 or 90 min appears to lead to both CNT damage and demixing mechanisms as shown in Figure 14. This demixing leads to some reagglomeration of the CNTs in the polymer matrix, and in combination to CNT damage induced by the excessive sonication leads to a deterioration of the CNT network during mixing and a subsequent reduction in nanocomposite properties.

5 | CONCLUSIONS

While the literature suggests that CNTs can be either damaged or demixed during processing, several complementary techniques presented in the current study suggest that multiple mechanisms are likely activated at sonication times that are longer than the optimum (30 min for this PCL/CNT nanocomposite system). For example, results from optical analysis and shear-induced crystallization suggest that the CNT agglomerate sizes monotonically decrease as the Stage 1 sonication time continues to increase. On the other hand, the homogeneity of the CNT spatial distributions as represented by the electrical conductivity and the mixing index values indicate an optimal Stage 1 mixing time for the system. In addition, UV–vis spectra indicate that samples subjected to longer Stage 1 sonication exhibit demixing or rebundling of CNTs at long times. These optimal conditions are also reflected in the development of viscoelasticity as well as the tensile and electrical properties of the CNT/PCL nanocomposites, with these properties reaching maximum values at the optimal Stage 1 sonication time of 30 min. The documented demixing and reagglomeration that occurs at

longer sonication times in turn leads to the deterioration of the mechanical and electrical properties. Furthermore, TEM images further appear to show direct evidence of CNT damage at longer Stage 1 sonication times.

Together, our findings suggest that both mechanisms of demixing and damage of the CNTs coexist at longer than optimum sonication times. The inferences from these multiple characterization techniques clearly show the negative impact of excessive ultrasonication on the dispersion and distribution of the CNTs and emphasize the importance of finding the optimum mixing conditions.

ACKNOWLEDGMENT

This research project used microscopy resources within the Laboratory for Multiscale Imaging at Stevens Institute of Technology.

ORCID

Jayadurga Iyer Ganapathi https://orcid.org/0000-0002-5923-5440
Stephanie S. Lee https://orcid.org/0000-0003-0964-6353
Dilhan M. Kalyon https://orcid.org/0000-0003-2066-0359
Frank T. Fisher https://orcid.org/0000-0003-4476-5040

REFERENCES

[1] P.-C. Ma, N. A. Siddiqui, G. Marom, J.-K. Kim, *Compos. Part A* **2010**, *41*, 1345.
[2] B. P. Grady, *Macromol. Rapid Commun.* **2010**, *31*, 247.
[3] S. Pegel, P. Pötschke, G. Petzold, I. Alig, S. M. Dudkin, D. Lellinger, *Polymer* **2008**, *49*, 974.
[4] Z. Spitalsky, D. Tasis, K. Papagelis, C. Galiotis, *Prog. Polym. Sci.* **2010**, *35*, 357.
[5] P. Alafogianni, K. Dassios, S. Farmaki, S. Antiohos, T. Matikas, N.-M. Barkoula, *Colloids Surf. A* **2016**, *495*, 118.
[6] H. Wang, *Curr. Opin. Colloid Interface Sci.* **2009**, *14*, 364.
[7] S. Giordani, S. D. Bergin, V. Nicolosi, S. Lebedkin, M. M. Kappes, W. J. Blau, J. N. Coleman, *J. Phys. Chem. B* **2006**, *110*, 15708.
[8] Q. Cheng, S. Debnath, E. Gregan, H. J. Byrne, *J. Phys. Chem. C* **2010**, *114*, 8821.
[9] H. Yu, S. Hermann, S. E. Schulz, T. Gessner, Z. Dong, W. J. Li, *Chem. Phys.* **2012**, *408*, 11.
[10] G. Gkikas, N.-M. Barkoula, A. Paipetis, *Compos. Part B* **2012**, *43*, 2697.
[11] A. Montazeri, M. Chitsazzadeh, *Mater. Des.* **1980**-2015, *2014*, 500.
[12] K. Lu, R. Lago, Y. Chen, M. Green, P. Harris, S. Tsang, *Carbon* **1996**, *34*, 814.
[13] G. Pagani, M. J. Green, P. Poulin, M. Pasquali, *Proc. Natl. Acad. Sci. U.S.A* **2012**, *109*, 11599.
[14] T. Liu, S. Luo, Z. Xiao, C. Zhang, B. Wang, *J. Phys. Chem. C* **2008**, *112*, 19193.
[15] F. Hennrich, R. Krupke, K. Arnold, J. A. Rojas Stütz, S. Lebedkin, T. Koch, T. Schimmel, M. M. Kappes, *J. Phys. Chem. B* **2007**, *111*, 1932.
[16] Y. Y. Huang, E. M. Terentjev, *Polymers* **2012**, *4*, 275.
[17] P.-C. Ma, S.-Y. Mo, B.-Z. Tang, J.-K. Kim, *Carbon* **2010**, *48*, 1824.
[18] S. Vural, K. B. Dikovics, D. M. Kalyon, *Soft Matter* **2010**, *6*, 3870.
[19] I. Alig, P. Pötschke, D. Lellinger, T. Skipa, S. Pegel, G. R. Kasaliwal, T. Villmow, *Polymer* **2012**, *53*, 4.
[20] T. McNally, P. Pötschke, *Polymer-Carbon Nanotube Composites*, Elsevier, Cambridge, UK **2011**.
[21] A. Wurm, D. Lellinger, A. A. Minakov, T. Skipa, P. Pötschke, R. Nicula, I. Alig, C. Schick, *Polymer* **2014**, *55*, 2220.
[22] I. Küçük, H. Gevgilili, D. M. Kalyon, *J. Rheol.* **2013**, *57*, 1491.
[23] J. Li, P. C. Ma, W. S. Chow, C. K. Tow, B. Z. Tang, J. K. Kim, *Adv. Funct. Mater.* **2007**, *17*, 3207.
[24] J. Iyer Ganapathi, F. T. Fisher, D. M. Kalyon, *J. Polym. Sci. Part B: Polym. Phys.* **2016**, *54*, 2254.
[25] J. Iyer Ganapathi, D. M. Kalyon, F. T. Fisher, *J. Appl. Polym. Sci.* **2017**, *134*, 44681.
[26] S. Rahatekar, K. Koziol, S. Butler, J. Elliott, M. Shaffer, M. Mackley, A. Windle, *J. Rheol.* **2006**, *50*, 599.
[27] R. G. Larson, *The Structure and Rheology of Complex Fluids*, Vol. 150, Oxford University Press, New York **1999**.
[28] J. Njuguna, O. A. Vanli, R. Liang, *J. Spectro.* **2015**, *2015*, 463156.
[29] N. Grossiord, O. Regev, J. Loos, J. Meuldijk, C. E. Koning, *Anal. Chem.* **2005**, *77*, 5135.
[30] J. Yu, N. Grossiord, C. E. Koning, J. Loos, *Carbon* **2007**, *45*, 618.
[31] R. Rastogi, R. Kaushal, S. Tripathi, A. L. Sharma, I. Kaur, L. M. Bharadwaj, *J. Colloid Interface Sci.* **2008**, *328*, 421.
[32] J. Rausch, R.-C. Zhuang, E. Mäder, *Compos. Part A* **2010**, *41*, 1038.
[33] G. Pircheraghi, R. Foudazi, I. Manas-Zloczower, *Powder Technol.* **2015**, *276*, 222.
[34] A. Sobolkina, V. Mechtcherine, V. Khavrus, D. Maier, M. Mende, M. Ritschel, A. Leonhardt, *Cem. Concr. Compos.* **2012**, *34*, 1104.
[35] L. Hui, R. Smith, X. Wang, J. Nelson, L. Schadler, Annual Report Conf. Electrical Insulation and Dielectric Phenomena, IEEE: **2008**; pp 317–320.
[36] D. Kim, J. S. Lee, C. M. Barry, J. L. Mead, *Microsc. Res. Tech.* **2007**, *70*, 539.
[37] B. Lively, P. Smith, W. Wood, R. Maguire, W.-H. Zhong, *Compos. Part A* **2012**, *43*, 847.
[38] Z. Luo, J. Koo, *J. Microsc.* **2007**, *225*, 118.
[39] S. R. Bakshi, R. G. Batista, A. Agarwal, *Compos. Part A* **2009**, *40*, 1311.
[40] H. Khare, D. Burris, *Polymer* **2010**, *51*, 719.
[41] A. Yazdanbakhsh, Z. Grasley, B. Tyson, R. K. A. Al-Rub, *Compos. Part A* **2011**, *42*, 75.
[42] Y.-H. Chen, G.-J. Zhong, J. Lei, Z.-M. Li, B. S. Hsiao, *Macromolecules* **2011**, *44*, 8080.
[43] G. Mago, F. T. Fisher, D. M. Kalyon, *Macromolecules* **2008**, *41*, 8103.
[44] Z. Tadmor, C. G. Gogos, *Principles of Polymer Processing*, 2nd ed., John Wiley & Sons, Hoboken, NJ **2013**.
[45] J. M. McKelvey, *Polymer Processing*, John Wiley & Sons, New York, NY **1962**.
[46] R. Yazici, D. Kalyon, *Rubber Chem. Technol.* **1993**, *66*, 527.

[47] P. Danckwerts, *Appl. Sci. Res. Sect A* **1952**, *3*, 279.
[48] M. Erol, D. Kalyon, *Int. Polym. Process.* **2005**, *20*, 228.
[49] D. M. Kalyon, D. Dalwadi, M. Erol, E. Birinci, C. Tsenoglu, *Rheol. Acta* **2006**, *45*, 641.
[50] M.-F. Yu, O. Lourie, M. J. Dyer, K. Moloni, T. F. Kelly, R. S. Ruoff, *Science* **2000**, *287*, 637.
[51] B. Peng, M. Locascio, P. Zapol, S. Li, S. L. Mielke, G. C. Schatz, H. D. Espinosa, *Nat. Nanotechnol.* **2008**, *3*, 626.
[52] J. P. Straley, *J. Phys. C: Solid State Phys.* **1976**, *9*, 783.
[53] D. Stauffer, A. Aharony, *Introduction to Percolation Theory*, CRC Press, London, UK **1994**.
[54] C. A. Mitchell, R. Krishnamoorti, *Macromolecules* **2007**, *40*, 1538.

How to cite this article: Iyer Ganapathi J, Lee SS, Kalyon DM, Fisher FT. Impact of ultrasonication on carbon nanotube demixing and damage in polymer nanocomposites. *J Appl Polym Sci*. 2020;49370. https://doi.org/10.1002/app.49370